Optical vortices in antiguides

Lorenzo Marrucci,[1,2,*] Noel F. Smyth,[3] and Gaetano Assanto[4]

[1]*Dipartimento di Fisica, Università di Napoli "Federico II," Complesso di Monte S. Angelo, Napoli 80126, Italy*

[2]*CNR-SPIN, Complesso Universitario di Monte S. Angelo, Napoli 80126, Italy*

[3]*School of Mathematics, University of Edinburgh, Edinburgh, Scotland, EH9 3JZ, UK*

[4]*NooEL—Nonlinear Optics and OptoElectronics Lab, University "Roma Tre," Rome 00146, Italy*

**Corresponding author: marrucci@na.infn.it*

Received March 6, 2013; accepted April 1, 2013;
posted April 8, 2013 (Doc. ID 186557); published May 7, 2013

We address the question of whether an optical vortex can be trapped in a dielectric structure with a core of a lower refractive index than the cladding—namely an antiguide. Extensive numerical simulations seem to indicate that this inverse trapping of a vortex is not possible, at least in straightforward implementations. Yet, the interaction of a vortex beam with a curved antiguide produces interesting effects, namely a small but finite displacement of the optical energy center-of-mass and the creation of a symmetrical vortex–antivortex pair on the exterior of the antiguide.

OCIS codes: (050.4865) Optical vortices; (130.2790) Guided waves; (260.6042) Singular optics.
http://dx.doi.org/10.1364/OL.38.001618

Analogies between different physical systems can be an important inspiration for conceiving new effects. Among them, swapping the roles of light and matter has been rather fruitful. For example, it is well known that in transparent media, light can be trapped in regions of a higher refractive index, such as in the core of standard waveguides [1]. Such trapping occurs in the transverse coordinates only, relative to the waveguide. Exchanging the roles of light and matter, we are naturally led to the concept of optical tweezers, which can trap small material particles in regions of higher light intensity [2,3]. In some sense, both effects stem from the same fundamental interaction between light and matter, that is, photon elastic scattering.

Optical tweezers work when the particles have a refractive index higher than the surrounding fluid. Conversely, when the particles have a lower index, they are repelled by the most intense regions of a bell-shaped beam. On the other hand, such particles can be trapped by means of doughnut beams, e.g., vortex beams with a central hole in the intensity distribution [4].

Now, exchanging the roles of light and matter, one might speculate that an optical vortex could be trapped (in the transverse plane) by a dielectric cylindrical structure having a core of lower refractive index than the cladding, i.e., an antiguide for brevity. If the antiguide is curved, then, one might be able to bend the vortex path and steer the light surrounding the vortex as well, since the doughnut is associated with a form of continuous rotation of optical energy around the vortex axis where the phase singularity is located. Such a rotation might tie the optical field of the doughnut to the axial singularity and force the light to follow the waveguide, at least in part, by being refracted sideways. In this Letter, we aim at testing these ideas using numerical experiments.

Light beams endowed with a vortex on axis carry orbital angular momentum (OAM) and have been the subject of intense studies in the last 20 years [5]. In particular, their interaction with inhomogeneous, anisotropic, or nonlinear optical media has been attracting increasing attention [6–16]. One of the simplest examples of such vortex beams is the Laguerre–Gauss mode with the radial number $p = 0$, which has the following expression in the focal plane:

$$u(r,\theta) = a r^{|m|} e^{-\frac{r^2}{w^2} + im\theta}. \tag{1}$$

Here (r,θ) are polar coordinates in the transverse plane (x,y), z is the propagation coordinate, w is the beam waist, a is an amplitude constant (unimportant in a linear analysis), and m is the integer winding number or vortex charge. m also quantifies the OAM per photon carried by the beam in units of $\hbar$.

For the wave propagation, we adopt the slowly varying envelope approximation. In dimensionless coordinates, we solve the paraxial Helmholtz equation:

$$i\frac{\partial u}{\partial z} + \frac{1}{2}\nabla_T^2 u + 2G(x,y,z)u = 0. \tag{2}$$

Here u is the complex envelope of the wave, ∇_T^2 the transverse Laplacian in x and y and G a function determined by the refractive index distribution $n(x,y,z)$ defining the guide. A longitudinal length scale L, which can be chosen arbitrarily for normalization, gives the units of the z coordinate. The transverse length $L_T = \sqrt{L\lambda/(2n_0\pi)}$ gives the units of the transverse x and y coordinates and the waist w, with λ the vacuum wavelength and n_0 the asymptotic refractive index of the surrounding medium (cladding). The function G giving the waveguide index profile is

$$G = \frac{\pi(n^2 - n_0^2)L}{2n_0\lambda} \approx \pi(n - n_0)\frac{L}{\lambda}, \tag{3}$$

where the approximate equality holds for small index variations.

In our simulations, we launch a beam defined by Eq. (1) at the input plane $z = 0$ into a curved graded-index waveguide with the Gaussian index distribution:

$$G(x,y,z) = Ae^{-\frac{y^2+[x-S(z)]^2}{W^2}}, \tag{4}$$

where $S(z) = X + R - \sqrt{R^2 - z^2}$ is the waveguide axis position versus z. The function $S(z)$ defines the waveguide bend shape, which in dimensionless units is a circular arc lying within the plane (x, z) of radius of curvature R and initial position X. The constant A gives the maximum waveguide depth in terms of the refractive index change and length scale L. For negative A the guide anticore has a lower refractive index than the surrounding, infinitely extended, cladding.

We first investigate the case $m = 1$, which is known to be the most stable case, because the vortex has the minimum possible charge (and OAM). Hence, it can neither spontaneously split into separate vortices of smaller charge, nor can it vanish owing to the conservation of the total topological charge. In a standard waveguide (positive A) the vortex can be confined by the refractive potential, consistent with previous studies on vortex stabilization by means of nonlocal spatial solitons [6,10,11,17]. In a curved positive waveguide, the vortex path can bend, undergoing profile distortions, vortex–antivortex pair generation, and radiation losses related to the curvature and to the waveguide core size relative to the input beam. However, it retains its global phase singularity located in the main beam, as illustrated, for example, in Fig. 1. The vortex behavior in an antiguide is displayed in Fig. 2. As the vortex propagates in the plane $(x, y = 0, z)$ an intensity hole appears to follow the antiguide axis, suggesting that the vortex is indeed being guided. However, a secondary hole, less visible, propagates straight [Fig. 1(a)]. This is more visible in the output intensity distribution, illustrated in Fig. 1(c). To distinguish between these, one needs to look at the optical phase distribution in the transverse plane (x, y) [Fig. 1(d)]. Clearly, the vortex is associated with the hole which propagates straight without significant transverse displacement with respect to the input. The second hole, following the bend, is due to light expelled from the antiguide. Therefore, there is no significant vortex trapping by the antiguide. Nevertheless, some interesting observations are in order.

First, the antiguide is found to push the light energy located on the right-hand side of the core, i.e., the side toward which the guide is curved. This can be clearly appreciated in the output intensity distribution, shown in Fig. 2(c) and is quantified in Fig. 2(b), which graphs the variation of intensity peak position and of the weighed average position of the light, as defined by

$$\langle x \rangle = \frac{\int_{-\infty}^{\infty}\int_{-\infty}^{\infty} x|u|^2 \mathrm{d}x\mathrm{d}y}{\int_{-\infty}^{\infty}\int_{-\infty}^{\infty} |u|^2 \mathrm{d}x\mathrm{d}y}. \quad (5)$$

The latter is the center-of-mass of the intensity distribution. The intensity peak essentially follows the antiguide, keeping just to the right of the core. The center-of-mass position is displaced by a much smaller, but finite amount.

Second, in the output section shown in Figs. 2(c) and 2(d), there is a pair of oppositely charged vortices ($m = +1$ and $m = -1$) generated by the refractive disturbance, located at $x \approx 50$ (close to the waveguide core) and $y \approx \pm 20$. It is important to note, albeit less clear, the collateral generation of oppositely charged vortices is also visible in Fig. 1(d) for the case of a positive waveguide.

Very similar behavior is observed for higher charge vortices. A representative example with $m = 3$ is shown in Fig. 3, but different $m > 1$ give qualitatively similar results. In comparison with the $m = 1$ case, the main

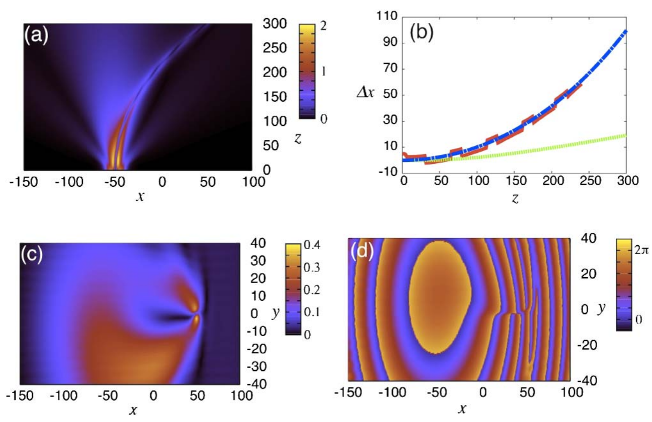

Fig. 1. Interaction of an optical vortex with charge $m = 1$ and a Gaussian positive waveguide. (a) Intensity evolution in a longitudinal cross-section (xz plane), with intensity-scale in false colors. (b) Displacement $\Delta x = x(z) - X$ of the waveguide center (dashed–dotted blue line), light intensity peak (solid red line) and average center (dotted green line) versus z. The location of the numerical maximum switches periodically between the symmetrical peaks on the two sides of the waveguide center. For $z > 230$ the maximum location is not stable due to the strong radiated energy. (c) Intensity distribution in a transverse cross-section at the exit plane $z = 300$. (d) Optical phase distribution in the same plane (phase-scale in false colors). The simulation parameters are: $A = 1$, $w = 10$, $W = 3$, $R = 500$, $X = -50$.

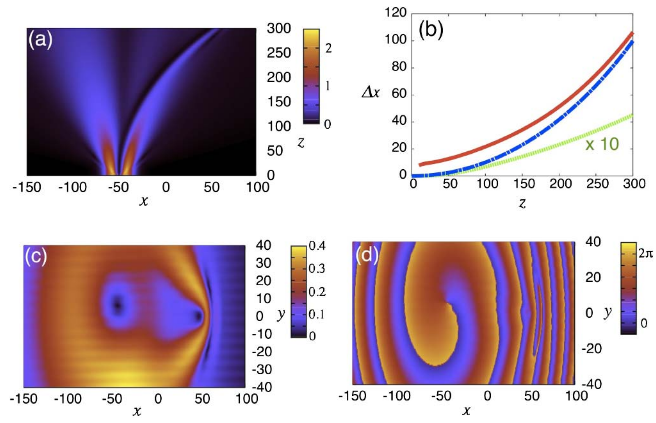

Fig. 2. Interaction of an optical vortex with charge $m = 1$ with a Gaussian antiguide. (a) Intensity evolution in a longitudinal cross-section (xz plane), with intensity scale in false colors. (b) Displacement $\Delta x = x(z) - X$ of the waveguide center (dashed–dotted blue line), intensity peak (red solid line), and average center (dotted green line) versus z (the latter is rescaled by a factor ×10). The red curve for small z is omitted because it switches randomly between the two symmetrical peaks on the two sides of the waveguide center. (c) Intensity distribution in a transverse cross-section at the exit plane $z = 300$. (d) Optical phase distribution in the same plane with phase scale in false colors. The simulation parameters are: $A = -1$, $w = 10$, $W = 3$, $R = 500$, and $X = -50$.

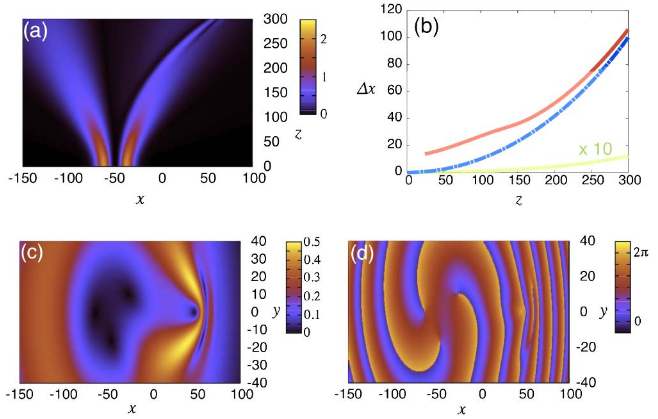

Fig. 3. Same as Fig. 2, but for an optical vortex with charge $m = 3$.

difference is that the central vortex, although not trapped by the waveguide, is perturbed enough to split into $|m|$ single charge vortices, which remain located in the central region. This is not unexpected, given the known instability of higher-order vortices.

We performed a number of tests by varying parameters, such as the ratio w/W between beam waist and guide size and the guide bend radius of curvature R and found no evidence of regimes in which the vortex is guided. This is not a formal proof negating the possibility of vortices being guided by an antiguide; very large radii R might indeed allow for vortex bending but, in such a limit, the long propagation distances required to observe a significant displacement would also result in large diffraction of the bright doughnut components, making the guiding effect nearly irrelevant. A possible route to counteract diffraction and bend vortices might consist of using positive waveguides with large R. We plan to explore this and other possibilities in future work.

In conclusion, our numerical experiments indicate that trapping an optical vortex by an antiguide is not possible, at least in those practical situations in which the trapping would be strong enough to operate over sufficiently short distances. As a consequence of the antiguide-vortex interaction, a small transverse shift of the optical energy and the generation of a vortex–antivortex pair on the antiguide exterior are induced, but no bend of the vortex path occurs. Higher-order vortices end up splitting into smaller vortices, due to their known structural instability. Further investigation will be required to assess the general validity of these results or identify exceptions in limiting cases.

This work was supported by the Royal Society of London, under Grant IE111560, and by the European Commission within the FET-Open Program of the 7th Framework Programme, under Grant No. 255914, PHORBITECH.

References

1. K. Okamoto, *Fundamentals of Optical Waveguides*, 2nd ed. (Academic,2006).
2. A. Ashkin, J. Dziedzic, J. Bjorkholm, and S. Chu, Opt. Lett. **11**, 288 (1986).
3. J. E. Molloy and M. J. Padgett, Contemp. Phys. **43**, 241 (2002).
4. K. T. Gahagan and G. A. Swartzlander, Jr., Opt. Lett. **21**, 827 (1996).
5. A. M. Yao and M. J. Padgett, Adv. Opt. Photon. **3**, 161 (2011).
6. V. I. Kruglov and R. A. Vlasov, Phys. Lett. A **111**, 401 (1985).
7. M. S. Soskin, V. N. Gorshkov, M. V. Vasnetsov, J. T. Malos, and N. R. Heckenberg, Phys. Rev. A **56**, 4064 (1997).
8. Y. S. Kivshar and B. Luther-Davies, Phys. Rep. **298**, 81 (1998).
9. M. S. Soskin and M. V. Vasnetsov, Prog. Opt. **42**, 219 (2001).
10. C. N. Alexeyev, A. V. Volyar, and M. A. Yavorsky, J. Opt. A **6**, S162 (2004).
11. A. S. Desyatnikov, Y. S. Kivshar, and L. Torner, Prog. Opt. **47**, 291 (2005).
12. A. Volyar, V. Shvedov, T. Fadeyeva, A. S. Desyatnikov, D. N. Neshev, W. Krolikowski, and Y. S. Kivshar, Opt. Express **14**, 3724 (2006).
13. S. Slussarenko, A. Murauski, T. Du, V. Chigrinov, L. Marrucci, and E. Santamato, Opt. Express **19**, 4085 (2011).
14. Y. V. Izdebskaya, A. S. Desyatnikov, G. Assanto, and Y. S. Kivshar, Opt. Express **19**, 21457 (2011).
15. R. Barboza, U. Bortolozzo, G. Assanto, E. Vidal, M. G. Clerc, and S. Residori, Phys. Rev. Lett. **109**, 143901 (2012).
16. A. Ambrosio, L. Marrucci, F. Borbone, A. Roviello, and P. Maddalena, Nat. Commun. **3**, 989 (2012).
17. Z. Xu, N. F. Smyth, A. A. Minzoni, and Y. S. Kivshar, Opt. Lett. **34**, 1414 (2009).